RARE METALS
Vol. 31, No. 3, Jun. 2012, p. 244
DOI: 10.1007/s12598-012-0499-2

Glass-forming ability and crystallization of Mg-Ni amorphous alloys with Y addition

LIU Liyan[a], TENG Xinying[a], WANG Yongjie[b], and LIU Teng[a]

[a] *School of Material Science and Engineering, University of Jinan, Jinan 250022, China*
[b] *School of Physics and Technology, University of Jinan, Jinan 250022, China*

Received 11 October 2011; received in revised form 12 December 2011; accepted 5 March 2012

Abstract

$Mg_{86.33}Ni_{13.67-x}Y_x$($x$=0, 1, 3, 6, 10) amorphous alloys were obtained by single-roller melt-spinning technique and the effect of Y addition on the glass forming ability(GFA), crystallization and micro-hardness of Mg-Ni alloys were studied. The results show that the GFA of $Mg_{86.33}Ni_{13.67-x}Y_x$($x$=0, 1, 3, 6, 10) is improved successfully with the Y addition. The highest GFA appeares at x=6, while the reduced glass transition temperature (T_{rg}) is 0.5225 and the supercooled liquid region(ΔT_x) is 42.06 K; the position of the main diffraction halo is different for the alloys, and the maximum of the main diffraction halo of alloys with x=0, 1, 3 corresponds to the main peaks of a metastable fcc-Mg_6Ni or fcc-Mg_6Ni + Ni-Y intermetallic phases, and for the alloys with x=6, 10, it corresponds to Mg-Y and Ni-Y intermetallic phases; the micro-hardness of the alloys is improved with Y additions, and the highest micro-hardness is obtained at x=6 at.%, which is 960 MPa.

Keywords: Mg-based amorphous alloy; glass forming ability; crystallization; micro-hardness

Amorphous alloy (also known as metallic glass) has attracted rapidly increasing attention due to their importance in understanding the fundamental science including nanocrystalline and quasicrystal as well as the potential engineering applications [1–2]. Compared with other bulk metallic glasses (BMGs), Mg-based BMGs are rapidly receiving attention due to their high specific strength, low cost and the abundance of Mg [3–4]. Therefore, a great deal of effort has been dedicated to searching Mg-based amorphous alloys with excellent glass-forming abilities (GFA). According to three empirical rules raised by Inoue [5], Mg-Tm-RE amorphous alloys can be obtained with high GFA. In case of Mg-Ni system, numerous studies have proved that Mg-Ni amorphous alloys exhibit excellent mechanical properties and corrosion resistance; meanwhile, Mg-Ni amorphous alloys can be used as an excellent hydrogen storage material [6–8]. In addition, rare earth elements have a strong influence on the rapidly solidified Mg-Ni amorphous alloys, and the GFA of the $Mg_{60}Ni_{23.6}La_{16.4}$ alloy with small amount of Y addition has been successfully improved by González *et al.* [9]. Till now, a number of Mg-Ni amorphous alloys have been fabricated successfully in the Mg-Ni-Re system for [10–14].

Mg-Cu amorphous alloys have been the focus of many studies due to their high GFA. Since Ni and Cu are close to each other in the periodic table of elements, a Mg-Ni alloy close to the eutectic composition ($Mg_{86.33}Ni_{13.67}$) was chosen and a small amount of Y was added to the alloy in this study. The purpose was to produce a Mg-based amorphous alloy with high GFA. The effect of Y addition on the GFA, the crystallization behavior and the mechanical properties of the rapidly quenched Mg-Ni amorphous alloy were studied.

1 Experimental

A Ni-Y intermediate alloy was firstly prepared by arc melting 99.99 wt.%Ni and 99.99 wt.%Y in argon atmosphere. The Ni-Y alloy was melted with 99.99 wt.% Mg by inductive melting under an argon atmosphere to obtain the pre-alloys ingots with nominal compositions of $Mg_{86.33}Ni_{13.67-x}Y_x$ (x=0, 1, 3, 6, 10). Using a single roller melt spinning apparatus, the pre-alloys were remelted in quartz tubes by high-frequency induction heating under a pure argon atmosphere and then melt-spun onto a copper roller to produce amorphous alloy ribbons. The circumferential speed of the roller was about 33 ms^{-1} and the ribbons were about 40 μm in thickness and 3 mm in width.

Phase identification of the samples was made by X-ray

Corresponding author: TENG Xinying **E-mail:** mse_tengxy@ujn.edu.cn

diffraction (XRD) using a Rigaku D/max with Cu Kα radiation. Thermal properties were investigated by differential thermal analysis (DTA, NETZSCH 409) technique at a heating rate of 20 K·min^{-1} (in flowing argon). The micro-hardness of the samples was studied with a HV-10B microscopic vickers hardness tester (load force is 4.9 N, t=10 s).

2 Results and discussion

2.1 Glass forming ability

Figure 1 shows the XRD patterns of $Mg_{86.33}Ni_{13.67-x}Y_x$ (with x=0, 1, 3, 6, 10) samples. It can be seen that all alloys synthesized exhibit broad humps at the position of about 2θ=30°~45°, indicating the formation of fully amorphous phase within XRD resolution.

It is interesting that the position of the main diffraction halo is different for the alloys. It is clearly seen that the position of the main diffraction halo shifts to small angles with the increasing of Y addition. The main diffraction halo of alloys with x=0, 1, 3 is at the position of about 2θ=38°, while the main diffraction halo of alloys with x=6, 10 is at the position of about 2θ=35°. According to the crystallization behavior in the following work, it can be concluded that the maximum of the main diffraction halo of the alloys with x=0, 1, 3 corresponds to the main peaks of a metastable fcc-Mg_6Ni or fcc-Mg_6Ni + Ni-Y intermetallic phases, while for the alloys with x=6, 10, it corresponds to Mg-Y and Ni-Y intermetallic phases. That fits well with the conclusion reported by Spassov *et al.* [15].

Figure 2(a) and (b) present the DTA curves of $Mg_{86.33}Ni_{13.67-x}Y_x$ (x=0, 1, 3, 6, 10) samples at a constant heating rate of 20 K·min^{-1}. All the samples exhibit typical thermodynamic character for amorphous phase, showing an obvious glass transition process with an endothermic peak for each sample and one exothermic peak or two exothermic peaks followed due to crystallization. Thermal properties of the alloys, including the values of glass transition temperature (T_g), the onset temperature of crystallization (T_x), and the melting temperature (T_m), were measured and listed in Table 1.

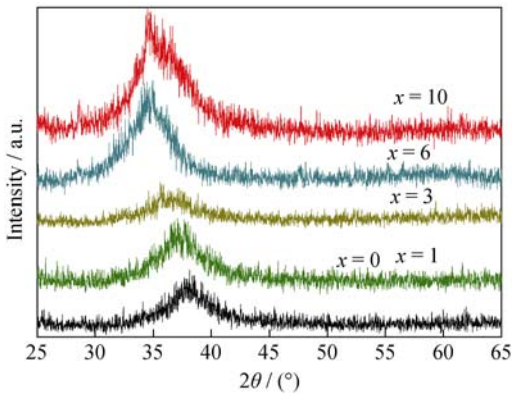

Fig. 1 XRD patterns of as-spun $Mg_{86.33}Ni_{13.67-x}Y_x$ alloys (with x=0, 1, 3, 6, 10)

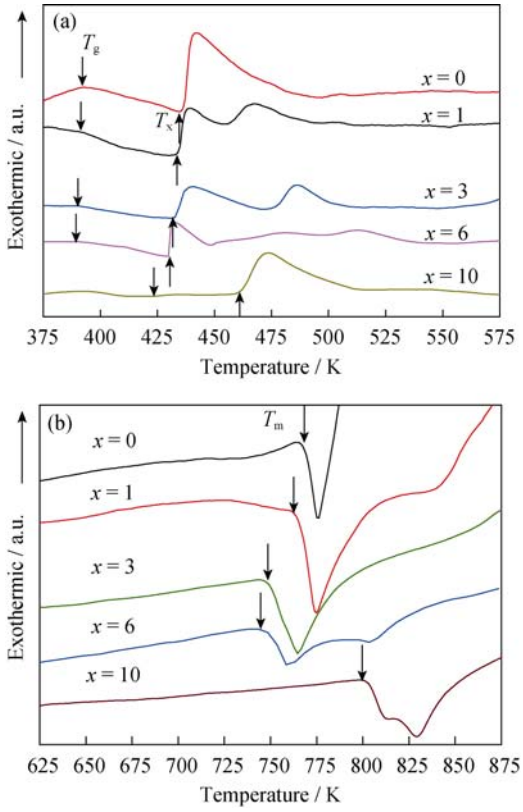

Fig. 2 DTA curves of $Mg_{86.33}Ni_{13.67-x}Y_x$($x$=0, 1, 3, 6, 10) amorphous alloys at a continuous heating rate of 20 K·min^{-1} (a) Glass transition curves; (b) Melting curves

Table 1 Thermodynamic data for $Mg_{86.33}Ni_{13.67-x}Y_x$($x$=0, 1, 3, 6, 10) amorphous alloys

x	T_g/K	T_x/K	T_m/K	ΔT_x/K	T_{rg}	K_{gl}
0	391.74	433.38	768.09	41.64	0.5100	0.1244
1	390.93	432.71	762.06	41.78	0.5130	0.1269
3	389.72	431.98	748.35	42.26	0.5208	0.1336
6	388.98	431.04	744.49	42.06	0.5225	0.1342
10	424.10	461.11	799.64	37.01	0.5304	0.1093

Reduced glass transition temperature T_{rg} ($T_{rg}=T_g/T_m$) and supercooled liquid region ΔT_x ($\Delta T_x=T_x-T_g$) can be used to evaluate GFA. All of the T_{rg} of the samples is larger than the critical value 0.2. It can be seen that the difference between T_g and T_x is not larger than 4 K for $Mg_{86.33}Ni_{13.67-x}Y_x$ alloys with x=0, 1, 3, 6, while the T_g and T_x for the alloy with x=10 increase obviously, which results in the little difference in ΔT_x for $Mg_{86.33}Ni_{13.67-x}Y_x$ alloys with x=0, 1, 3, 6, and a slight drop for the alloy with x=10 (in Fig. 3). On the other hand, the melting temperature T_m of the alloys is strongly dependent on Y content. With increasing Y content, the T_m of the alloys decreases from 768.09 K at x=0 down to 744.49 K at x=6, with the result that T_{rg} increases from 0.5100 at x=0 to 0.5225 at x=6. Meanwhile, although T_m increases up to 799.64 K at x=10, T_{rg} increases up to 0.5304 due to the greater increasing of T_g (as shown in Fig. 4). Thereby the best GFA is obtained at x=6 and x=10.The magnitude of supercooled liquid region ΔT_x is also usually used to evaluate thermal stability of amorphous alloy, which stands for ability of resistance to crystallization. It can be seen that the thermal stability of $Mg_{86.33}Ni_{13.67-x}Y_x$ alloys can be improved when Y content does not exceed 6 at.%.

K_{gl} is another important parameter to evaluate GFA, standing for tendency for formation of amorphous alloy. The larger the K_{gl}, the higher the GFA. The values of K_{gl} are given by the formula :

$$K_{gl}=(T_{x1}-T_g)/(T_m-T_x) \quad (1)$$

K_{gl} increases gradually at x=0, 1, 3, 6, then decreases significantly at x=10. The maximum of K_{gl} is at the composition with x=6, which demonstrates that the highest GFA is obtained at x=6(as shown in Fig. 4). The sequence is consistent with the tendency for ΔT_x.

According to comprehensive evaluation with T_{rg}, ΔT_x and K_{gl}, it can be concluded that the factors determining the GFA of alloys are complicated and the highest GFA appears at x=6 for $Mg_{86.33}Ni_{13.67-x}Y_x$ (x=0, 1, 3, 6, 10) amorphous alloys.

It also can be seen from Fig. 3 that the alloy with x=1 displays a single absorption peak with a smaller melting interval. The melting intervals of the alloys broaden gradually with Y addition, and double endothermic peaks appear at x=6, 10, which indicates that the ternary alloy of Mg-Ni-Y is deviated from the eutectic composition with increasing Y content.

On the basis of the principle of thermodynamics and summary of experimental results of amorphous alloy, Inoue has put forward three empirical rules for composition of alloys with high GFA and large ΔT_x [5]: (1) the alloys should belong to multicomponent systems consisting of more than three elements; (2) the difference in atomic size ratios among the three main constituent elements should be above 12% and (3) the elements should exhibit a negative heat of mixing. The three empirical rules can be accomplished for Mg-Ni-Y alloys. Formation of amorphous state is restricted by thermodynamic factors, so reducing Gibbs free energy ΔG will help improve stability of supercooled liquid phase and thermodynamic parameters so as to improve GFA of alloys. ΔG can be express by the formula:

$$(\Delta G=\Delta H-T\Delta S) \quad (2)$$

where ΔH is the negative heat of mixing, and ΔS is the entropy. It can be seen that increase of ΔS due to multicomponent systems and large difference in atomic size is useful to increase mismatch degrees of atomic arrangement; the larger ΔH between constituent elements is effective for improving solid-liquid surface energy, facilitating the decreasing of ΔG, which are resistant to crystallization and growth of crystalline phase. Viscosity of super-cooled liquid phase of the alloys will increase dramatically when temperature decreases, which retards atomic long-range rearrangement and improves GFA and thermal stability of amorphous alloys. In this work, the improvement of the GFA of the $Mg_{86.33}Ni_{13.67-x}Y_x$ alloys can be interpreted by the interplay between the degree of disorder of atoms in the alloys and their strong correlation behavior. As for the radius of Y atom (0.182 nm)

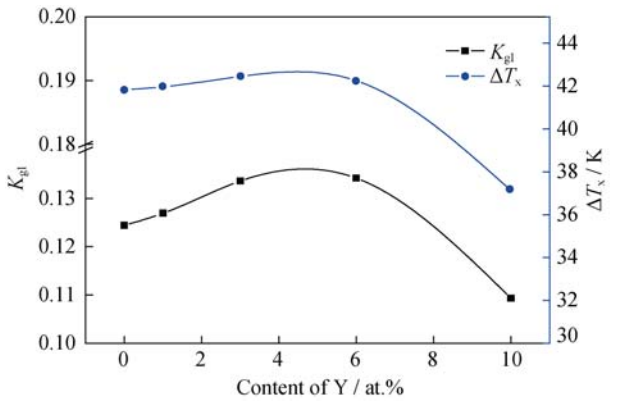

Fig. 3 K_{gl} and ΔT_x versus Y content

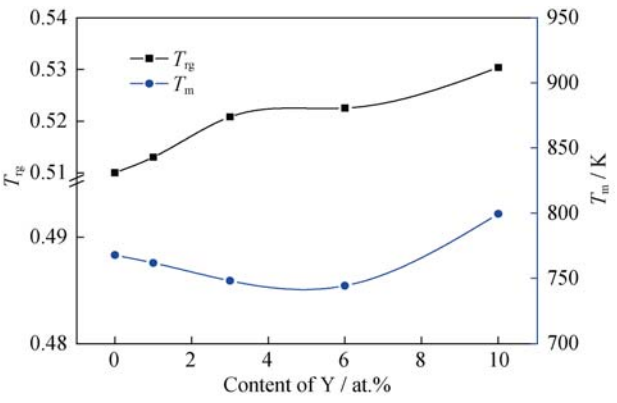

Fig. 4 T_{rg} and T_m versus Y content

is greater than Mg and Ni (0.160 and 0.125 nm respectively), and there is large negative heat of mixing and strong bond energy for Mg-Ni, Mg-Y and Ni-Y, as presented in Table 2, which makes atomic diffusion more difficult during growth of crystalline phase, leading to additional delay of the crystallization and growth process. So with Y addition, the GFA of the $Mg_{86.33}Ni_{13.67-x}Y_x$ alloys has been improved successfully. On the other hand, GFA of alloys is strongly sensitive to oxygen content. According to Xi *et al*. [16], RE elements can improve the GFA of Mg-based amorphous alloys due to the scavenging effect of oxygen impurities with the formation of innocuous RE oxides. The enthalpy of formation of Y_2O_3 (1905 kJ·mol^{-1}) is much larger than Mg_2O and NiO (601.6 kJ·mol^{-1} and 239.7 kJ·mol^{-1}, respectively) [9], so the formation of Y_2O_3 is more favourable and would be responsible for scavenging oxygen from the alloys. That reduces the damaging of oxygen on the GFA and improves the GFA effectively. However, excess Y additions can deteriorate the GFA and stability of the alloys due to the heterogeneous nucleation caused by the excess Y.

Table 2 Basic parameters of Mg, Ni, Y

Basic elements	Mg	Ni	Y
Atomic radius/nm	0.160	0.125	0.182
Constituent elements	Mg-Ni	Mg-Y	Ni-Y
Atomic radius difference/%	21.9	12.1	31.3
Enthalpy heat of mixing / (kJ·mol^{-1})	–13	–6	–97
Electronegativity	1.2	1.9	1.2

2.2 Crystallization

The structures of the samples after different heat treatments were studied by XRD in order to research the crystalline products of the alloys. The remarkable crystallization of the $Mg_{86.33}Ni_{13.67}$ alloy occurred after annealing above 423 K for 15 min, consisting only of the metastable phase Mg_6Ni. With further heating, the metastable phase Mg_6Ni transformed into the equilibrium Mg_2Ni and α-Mg crystalline phases(Fig. 5(a)). From Fig. 5(b), it can be seen that the XRD pattern of $Mg_{86.33}Ni_{12.67}Y_1$ alloy heated up to 443 K displayed obvious crystalline peaks superimposed on the amorphous diffraction peak, which are identified as face-centered cubic(fcc) Mg_6Ni and a small amount of Ni-Y intermetallics. No other crystalline phase was precipitated as the alloy is continuously heated up to 493 and 573 K, indicating that the Mg_6Ni phase in this alloy is stable up to 573 K. Two crystalline phases (Ni_7Y_2 and NiY) were detected firstly for the sample of the $Mg_{86.33}Ni_{10.67}Y_3$ alloy annealed for 15 min at 523 K(Fig. 5(c)), then Mg_6Ni phases appeared as the temperature increased up to 573 K. For $Mg_{86.33}Ni_{7.67}Y_6$ alloy(Fig. 5(d)), Ni_7Y_2 phases was observed firstly and then $Mg_{24}Y_5$ and some other Ni-Y compounds were precipitated after annealing for 15 min at 723 K. The crystalline products of the $Mg_{86.33}Ni_{3.67}Y_{10}$ alloy consisted only of Ni_7Y_2 and NiY_3 phases below 673 K. $Mg_{24}Y_5$ phases were observed until the alloy was annealed for 15 min at 723 K(Fig. 5(e)).

The XRD reveals a preferential orientation of Mg_6Ni and

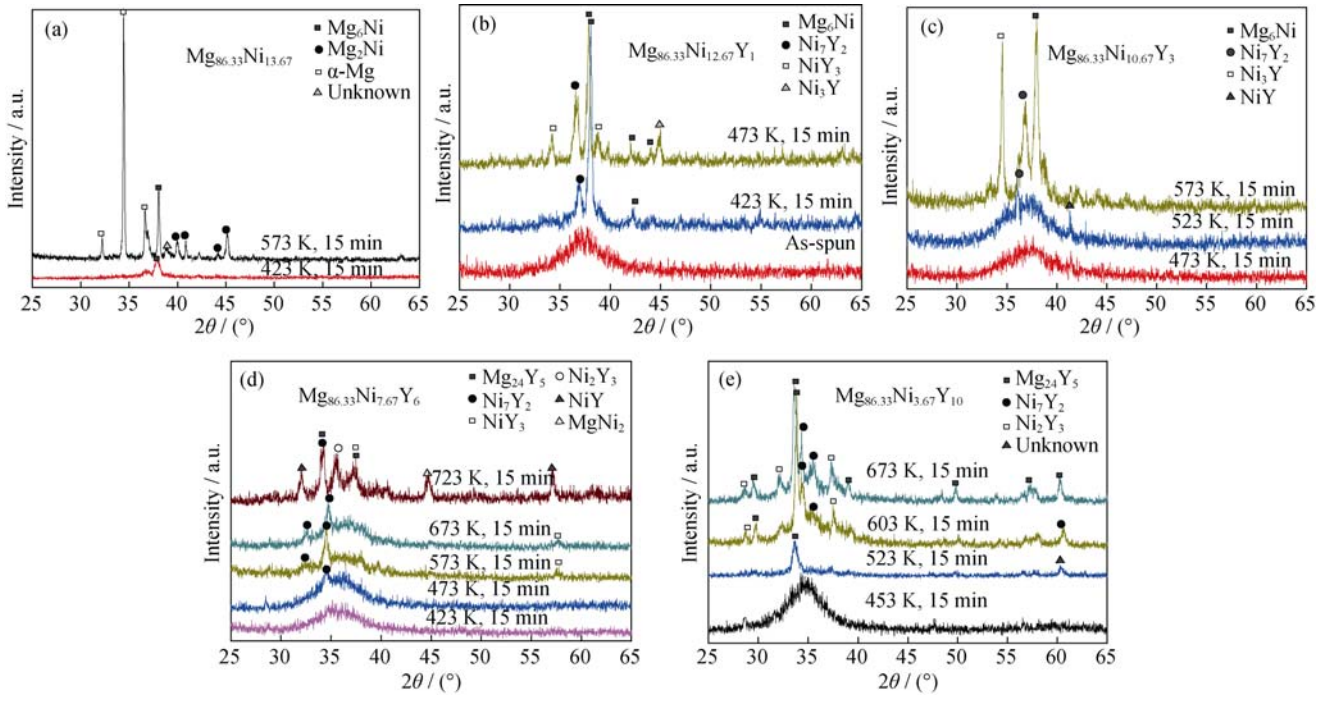

Fig. 5 XRD patterns of the as-annealed $Mg_{86.33}Ni_{13.67-x}Y_x$($x$=0, 1, 3, 6, 10) amorphous alloys

Ni-Y intermetallics (only Mg_6Ni for the alloy with x=0) for the alloys with x=0, 1 and 3, while the diffraction peak maximum is at the different position (about 35°) and corresponds to Mg-Y and Ni-Y intermetallics ($Mg_{24}Y_5$, Ni_7Y_2 mainly) for the alloys with x=6 and 10.

2.3 Mechanical properties

Figure 6 summarizes the change in the micro-hardness with different Y content for $Mg_{86.33}Ni_{13.67-x}Y_x$(with x=0, 1, 3, 6, 10) amorphous alloys. From Fig. 6 it can be seen that the micro-hardness of the alloys shows a tendency of rising firstly then decreasing rapidly. The increase in the micro-hardness is observed when Y content does not exceed 6 at.%, in which the micro-hardness increases from 917 to 960 MPa. With Y content further increasing(10 at.%), however, the micro-hardness decreases considerably (down to 903 MPa). For Mg-Ni system, addition of Y atoms with larger size can increase the mismatch degrees between the constituent atoms; on the other hand, the negative heat of mixing for Ni-Y is –97 kJ·mol^{-1}, which is much larger than Mg-Ni. Therefore, adequate addition of Y can strengthen the bond energy between the constituent atoms, increasing the ability of the resistance to deformation of the alloys, facilitating the increase of the micro-hardness. With the further increase of Y addition, Y atoms with larger size will be dominant in the constituent elements, so the mismatch degrees and the bond energy between the constituent atoms will be decreased, which leads to the decline of the micro-hardness.

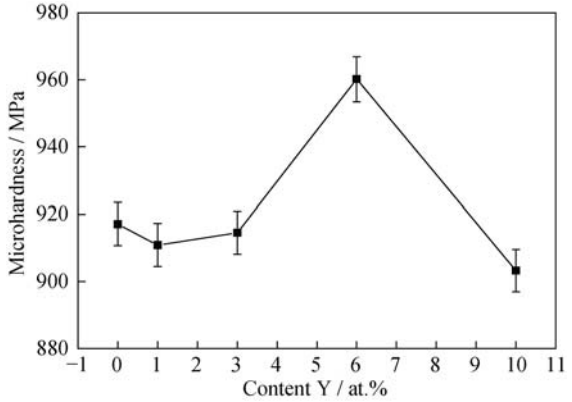

Fig. 6 Micro-hardness versus Y content for $Mg_{86.33}Ni_{13.67-x}Y_x$ (x=0, 1, 3, 6, 10) amorphous alloys

3 Conclusion

All the alloys of $Mg_{86.33}Ni_{13.67-x}Y_x$(with x=0, 1, 3, 6, 10) were obtained in the amorphous state by melt spinning, and the GFA of the alloys was improved with Y addition. $Mg_{86.33}Ni_{7.67}Y_6$ exhibited the highest GFA, indicating that Y has a strong influence on the GFA of rapidly solidified Mg-Ni amorphous alloys.

The position of the main diffraction halo is different for the alloys, and the maximum of the main diffraction halo of alloys with x=0, 1, 3 corresponds to metastable fcc- Mg_6Ni or fcc-Mg_6Ni + Ni-Y intermetallic phases, while for the alloys with x=6, 10, it corresponds to Mg-Y and Ni-Y intermetallic phases.

The micro-hardness of the $Mg_{86.33}Ni_{13.67-x}Y_x$(with x=0, 1, 3, 6, 10) amorphous alloys increases considerably with Y additions. The maximum degree of micro-hardness is obtained at x=6, which is 960 MPa.

Acknowledgment

This work was supported by the Award Fund for Outstanding Young Scientist in Shandong Province, China (No. BS2011CL004).

References

[1] Wang W.H., Bulk metallic glasses with functional physical properties, *Adv. Mater.*, 2009, **21** (45): 1.

[2] Jian S.R., Li J.B., Chen K.W., Jang Jason S.C., Juang J.Y., Wei P.J., and Lin J.F., Mechanical responses of Mg-based bulk metallic glasses, *Intermetallics*, 2010, **18** (10): 1930.

[3] Jean Louis Soubeyroux, and Sylvain Puech, Phases formation during heating of Mg-Cu-Ag-Y bulk metallic glasses, *Journal of Alloys and Compounds*, 2010, **495** (2): 330.

[4] Park E.S., Kyeong J.S., and Kim D.H., Enhanced glass forming ability and plasticity in Mg-based bulk metallic glasses, *Materials Science and Engineering A*, 2007, **449-451** : 225.

[5] Inoue A, Stabilization of metallic supercooled liquid and bulk amorphous alloys, *Acta Mater.*, 2000, **48** (1): 279.

[6] Zhang Y.H., Zhao D.L., Li B.W., Qi Y., Guo S.H., and Wang X.L., Hydrogen storage behaviours of nanocrystalline and amorphous $Mg_{20}Ni_{10-x}Co_x$ (x=0-4) alloys prepared by melt spinning, *Trans. Nonferrous Met. Soc. China*, 2010, **20** (3): 405.

[7] Siarhei Kalinichenka, Lars Rontzsch, Carsten Baehtz, and Bernd Kieback, Hydrogen desorption kinetics of melt-spun and hydrogenated $Mg_{90}Ni_{10}$ and $Mg_{80}Ni_{10}Y_{10}$ using in situ synchrotron, X-ray diffraction and thermogravimetry, *Journal of Alloys and Compounds*, 2010, **496** (1-2): 608.

[8] Wu D.C., Liang G.Y., Li L., and Wu H.B., Microstructural investigation of electrochemical hydrogen storage in amorphous Mg-Ni-La alloy, *Materials Science and Engineering B*, 2010, **175** (3): 248.

[9] González S., Figueroa I.A., and Todd I., Influence of minor

alloying addition on the glass-forming ability of Mg-Ni-La bulk metallic glasses, *Journal of Alloys and Compounds*, 2009, **484** (1-2): 612.

[10] Xu F., Du Y.L., Gao P., Han Z.D., Chen G., Wang S.Q., and Jiang J.Z., Crystallization of melt-spun $Mg_{63}Ni_{22}Pr_{15}$ amorphous alloy ribbon, *Journal of Alloys and Compounds*, 2007, **441** (1-2): 76.

[11] Lu Z.P., Liu C.T., and Li Y., Glass transition and crystallization of Mg-Ni-Nd metallic glasses studied by temperature-modulated DSC, *Intermetallics*, 2004, **12** (7-9): 869.

[12] Gonzalez S., Figueroa I.A., Zhao H., Davies H.A., Todd I., and Adeva P., Effect of mischmetal substitution on the glass-forming ability of Mg-Ni-La bulk metallic glasses, *Intermetallics*, 2009, **17** (11): 968.

[13] Perez P., Gonzalez S., and Garces G., Influence of partial replacement of cerium-rich mischmetal (CeMM) by yttrium on the crystallization and mechanical properties of amorphous $Mg_{80}Ni_{10}CeMM_{10}$ alloy, *Intermetallics*, 2007, **15** (3): 315.

[14] Perez P., Garces G., Gonzalez S., Nitsche H., Sommer F., and Adeva P., Change in mechanical properties during crystallization of amorphous $Mg_{83}Ni_9Y_8$, *Materials Science and Engineering A*, 2007, **462** (1-2): 211.

[15] Spassov T., Solsona P., Surinach S., and Baro M.D., Nanocrystallization in $Mg_{83}Ni_{17-x}Y_x$(x=0,7.5) amorphous alloys. *Journal of Alloys and Compounds*, 2002, **345** (1-2): 123.

[16] Xi X.K., Wang R.J., Zhao D.Q., Pan M.X., and Wang W.H., Glass-forming Mg-Cu-RE (RE=Gd, Pr, Nd, Tb, Y, and Dy) alloys with strong oxygen resistance in manufacturability, *Journal of Non-Crystalline Solids*, 2004, **344** (3): 105.